Supporting Information

Comparative Electromagnetic Shielding Performance of $Ti_3C_2T_x$-PVA Composites in Various Structural Forms: Compact Films, Hydrogels, and Aerogels

Shabbir Madad Naqvi[1], Tufail Hassan[1], Aamir Iqbal[1], Shakir Zaman[1], Sooyeong Cho[1], Noushad Hussain[1], Xiangmeng Kong[1], Zubair Khalid[1], Zhiwang Hao[1], Chong Min Koo[1,2,*]

[a]School of Advanced Materials Science and Engineering, Sungkyunkwan University, Seobu-ro 2066, Jangan-gu, Suwon-si, Gyeonggi-do, 16419 Republic of Korea.

[b]School of Chemical Engineering, Sungkyunkwan University, Seobu-ro 2066, Jangan-gu, Suwon-si, Gyeonggi-do, 16419 Republic of Korea.

*Corresponding author. Email: chongminkoo@skku.edu (C. M. K.)

Contents:

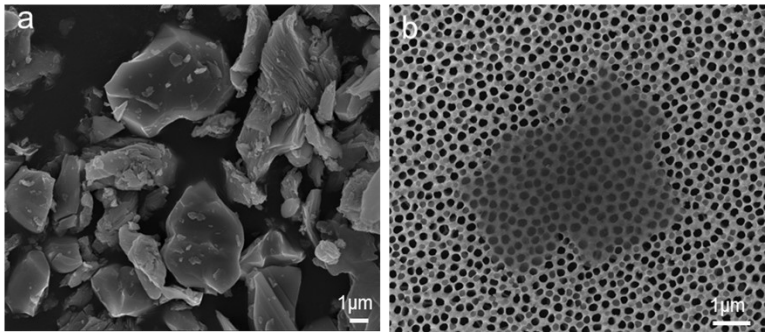

Figure S1. SEM images of (a) Ti_3AlC_2 MAX powders and (b) a single $Ti_3C_2T_x$ flake.

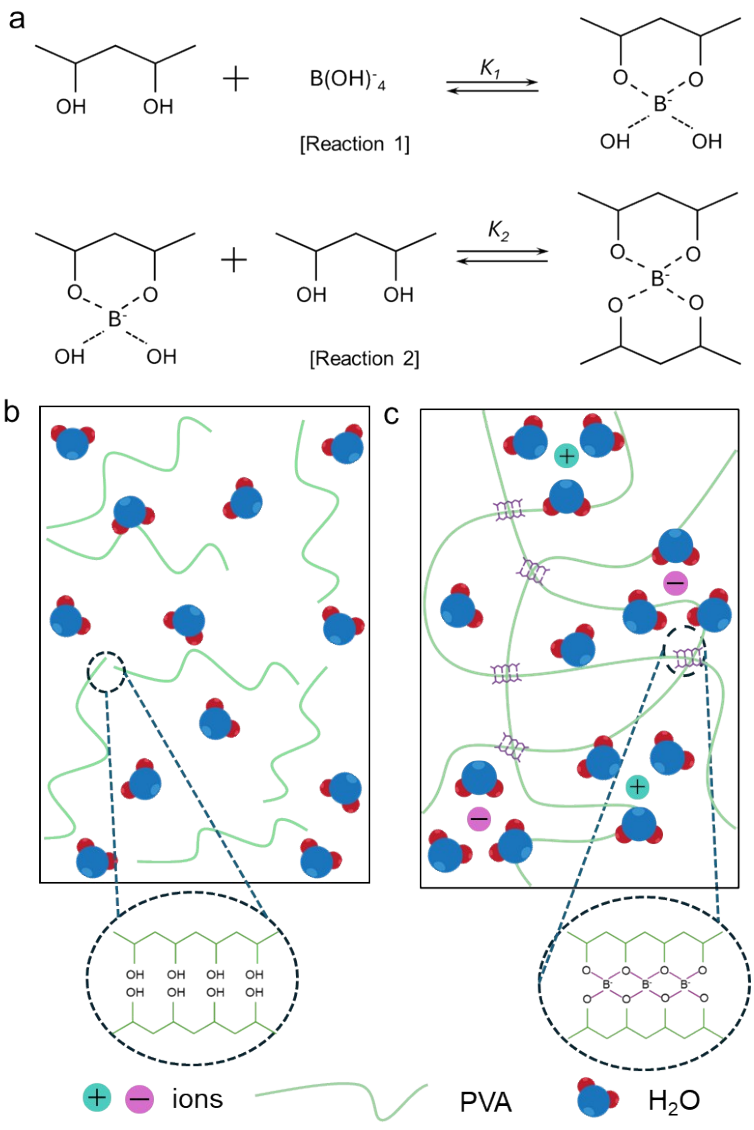

Figure S2. (a) PVA-borate crosslinking mechanism: reaction 1, monodiol complexation; and reaction 2, crosslink formation. Schematic illustration of bonding interactions (b) before and (c) after adding borax to a PVA aqueous solution.

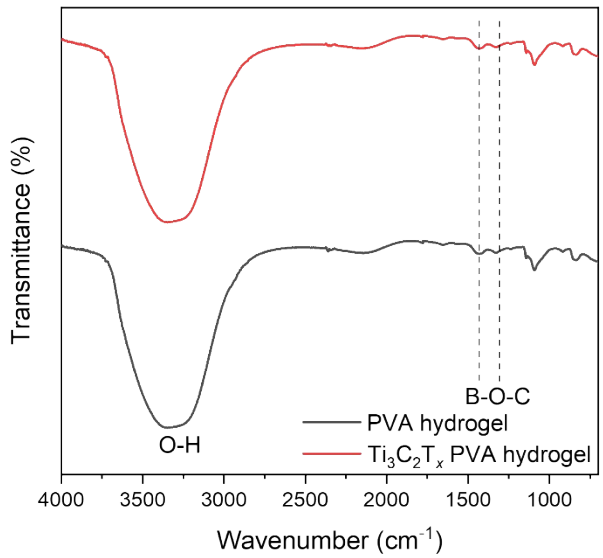

Figure S3. Fourier Transform Infrared spectroscopy spectra of PVA hydrogel, and $Ti_3C_2T_x$-PVA hydrogel.

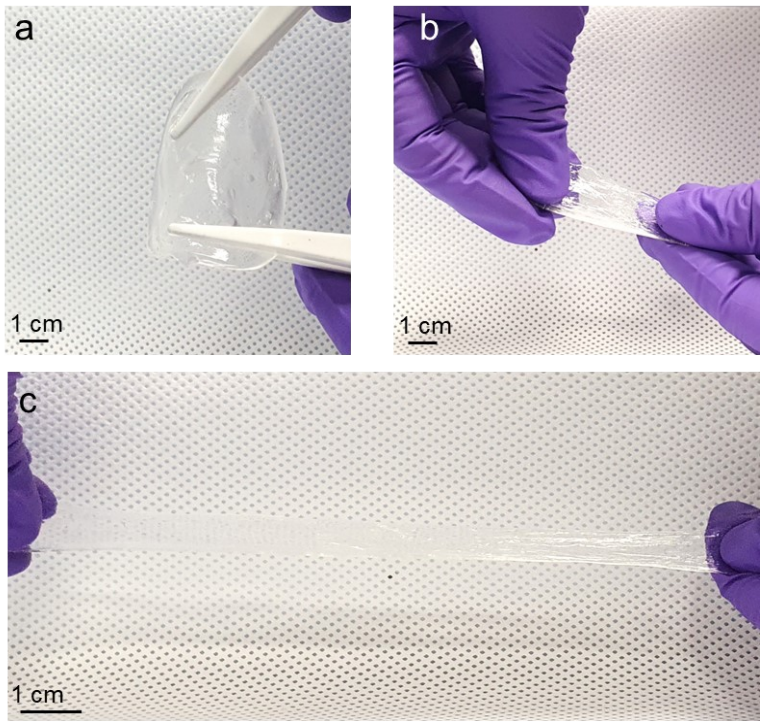

Figure S4. (a–c) Digital photographs of a PVA gel and its stretchable behavior.

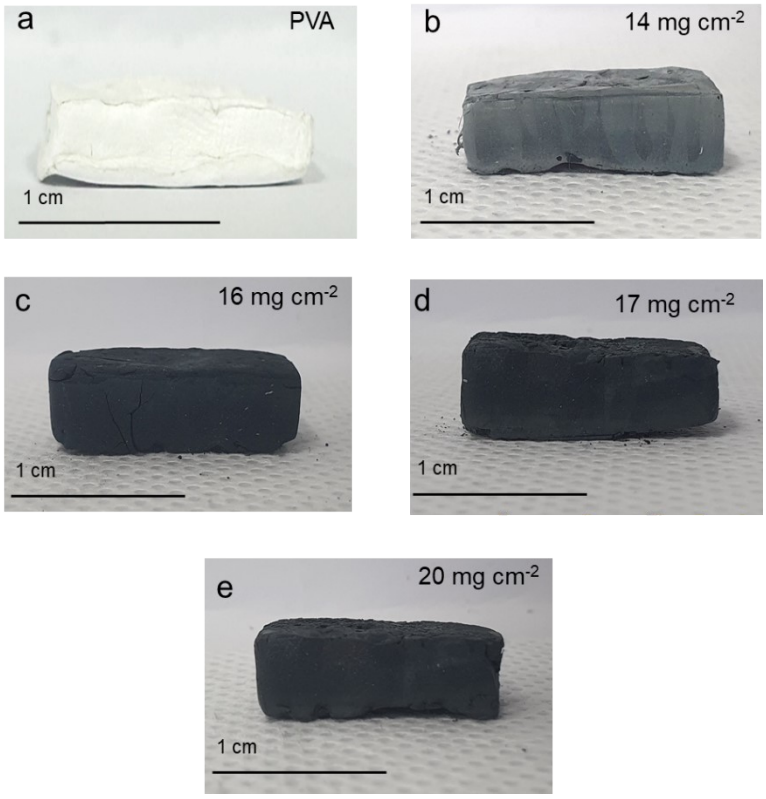

Figure S5. Digital photographs of $Ti_3C_2T_x$-PVA aerogels at various $Ti_3C_2T_x$ areal densities.

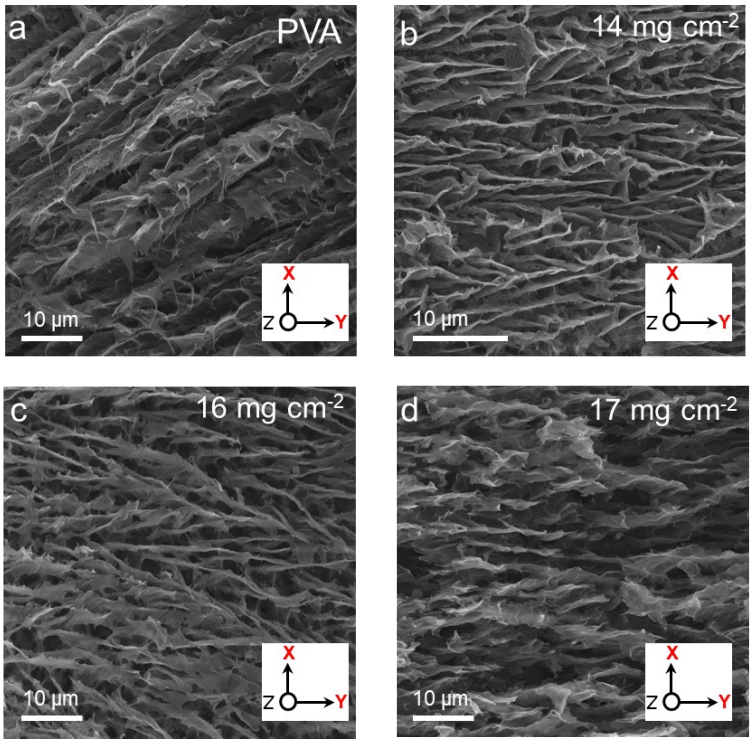

Figure S6. Cross-sectional SEM images in the XY direction of (a) PVA and (b–d) $Ti_3C_2T_x$-PVA aerogels at various $Ti_3C_2T_x$ areal densities.

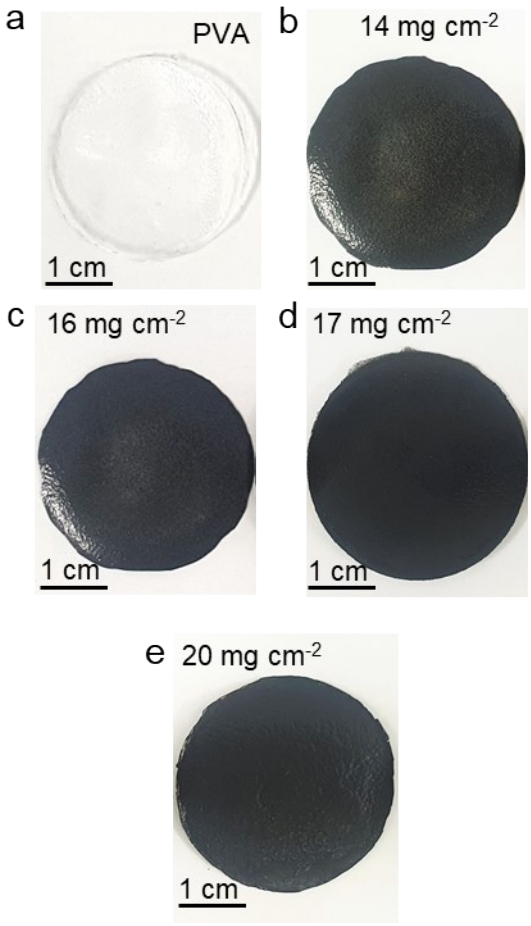

Figure S7. Digital photographs of (a) PVA and (b–e) $Ti_3C_2T_x$-PVA compact films at various $Ti_3C_2T_x$ areal densities.

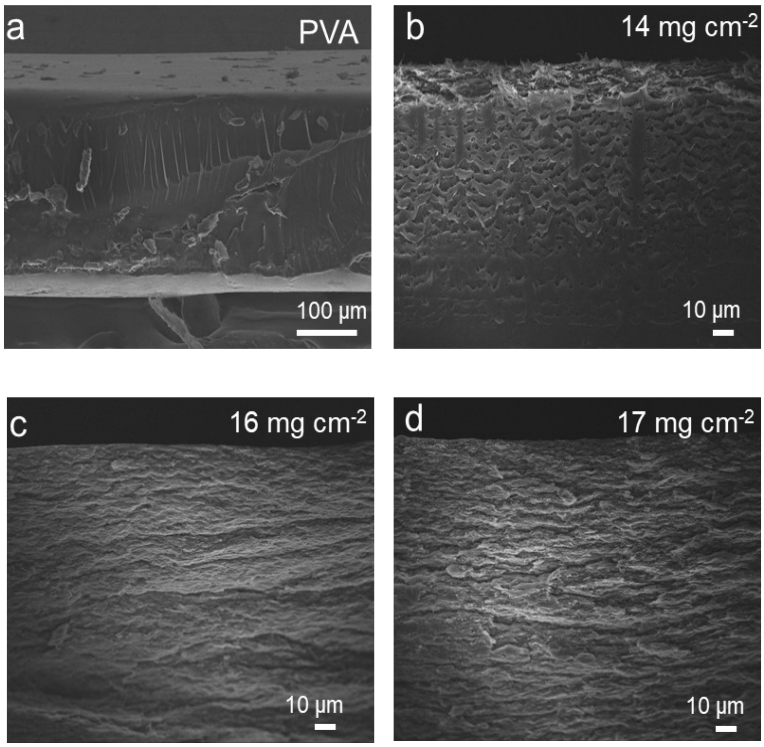

Figure S8. SEM images of (a) PVA and (b–d) $Ti_3C_2T_x$-PVA compact films at various $Ti_3C_2T_x$ areal densities.

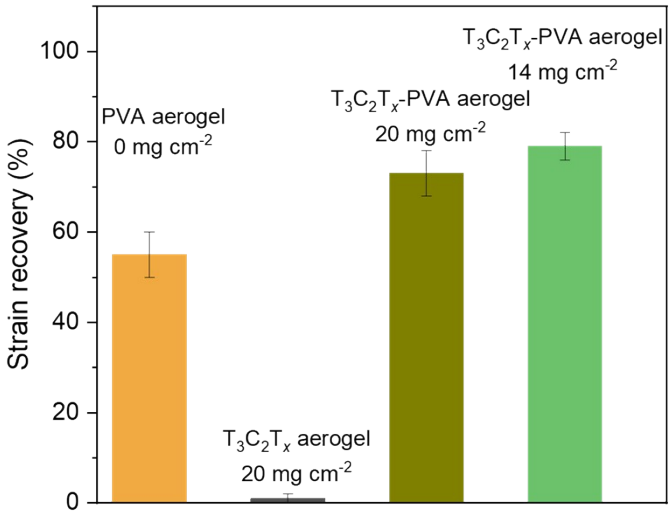

Figure S9. Strain recovery percentage of aerogels after applied compressive load is released.

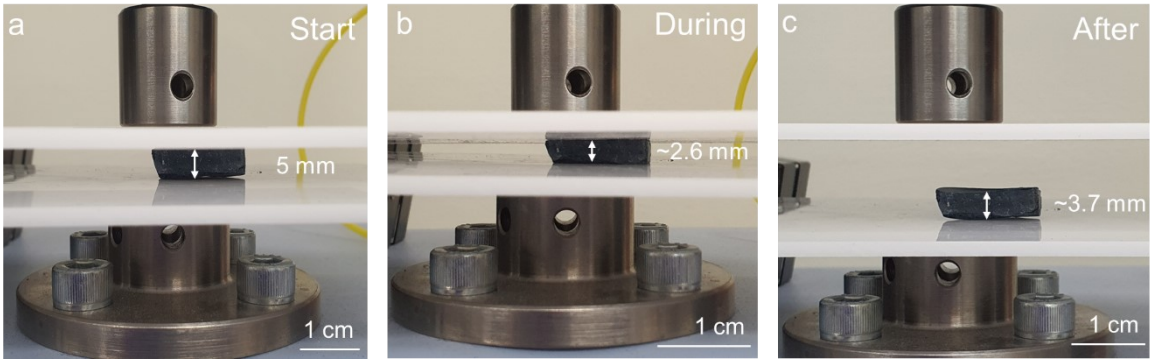

Figure S10. Digital photographs of the $T_3C_2T_x$-PVA aerogel (20 mg cm^{-2}) taken at the start (a), during the application of compressive stress (b), and after the removal of compressive stress (c).

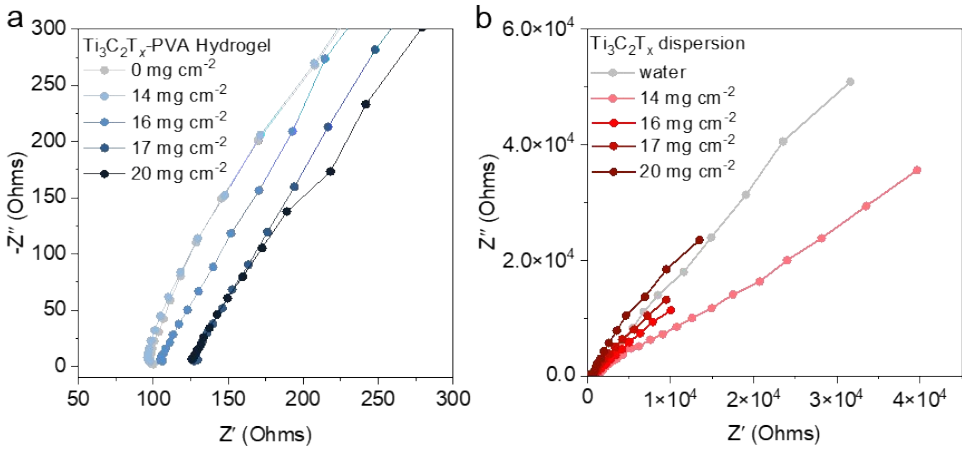

Figure S11. Nyquist plots for (a) $Ti_3C_2T_x$-PVA hydrogel and (b) $Ti_3C_2T_x$ dispersion in deionized water at various $Ti_3C_2T_x$ areal densities.

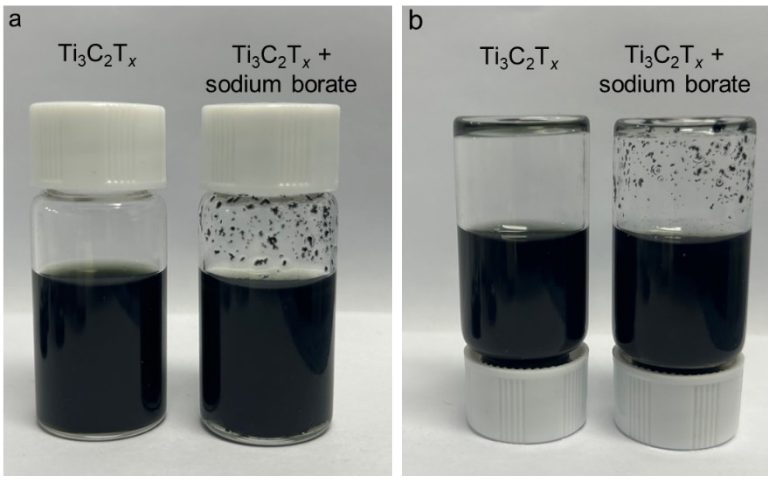

Figure S12. (a–b) Digital photographs of $Ti_3C_2T_x$ aqueous dispersions with and without sodium borate to highlight the coagulation behavior of the dispersion after the addition of sodium borate.

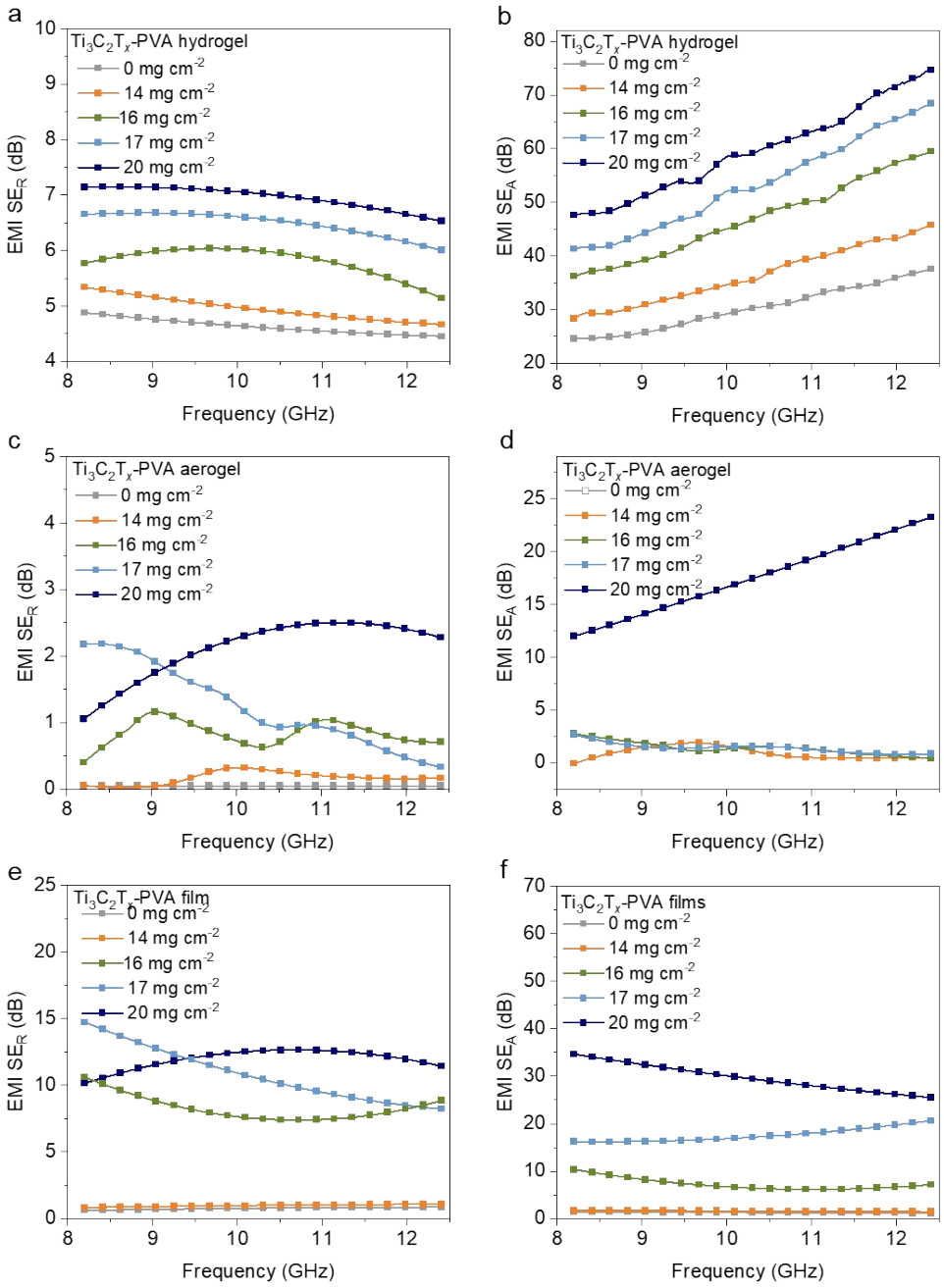

Figure S13. SE_R and SE_A for (a–b) $Ti_3C_2T_x$-PVA hydrogels, (c–d) $Ti_3C_2T_x$-PVA aerogels, and (e–f) $Ti_3C_2T_x$-PVA compact films, respectively.

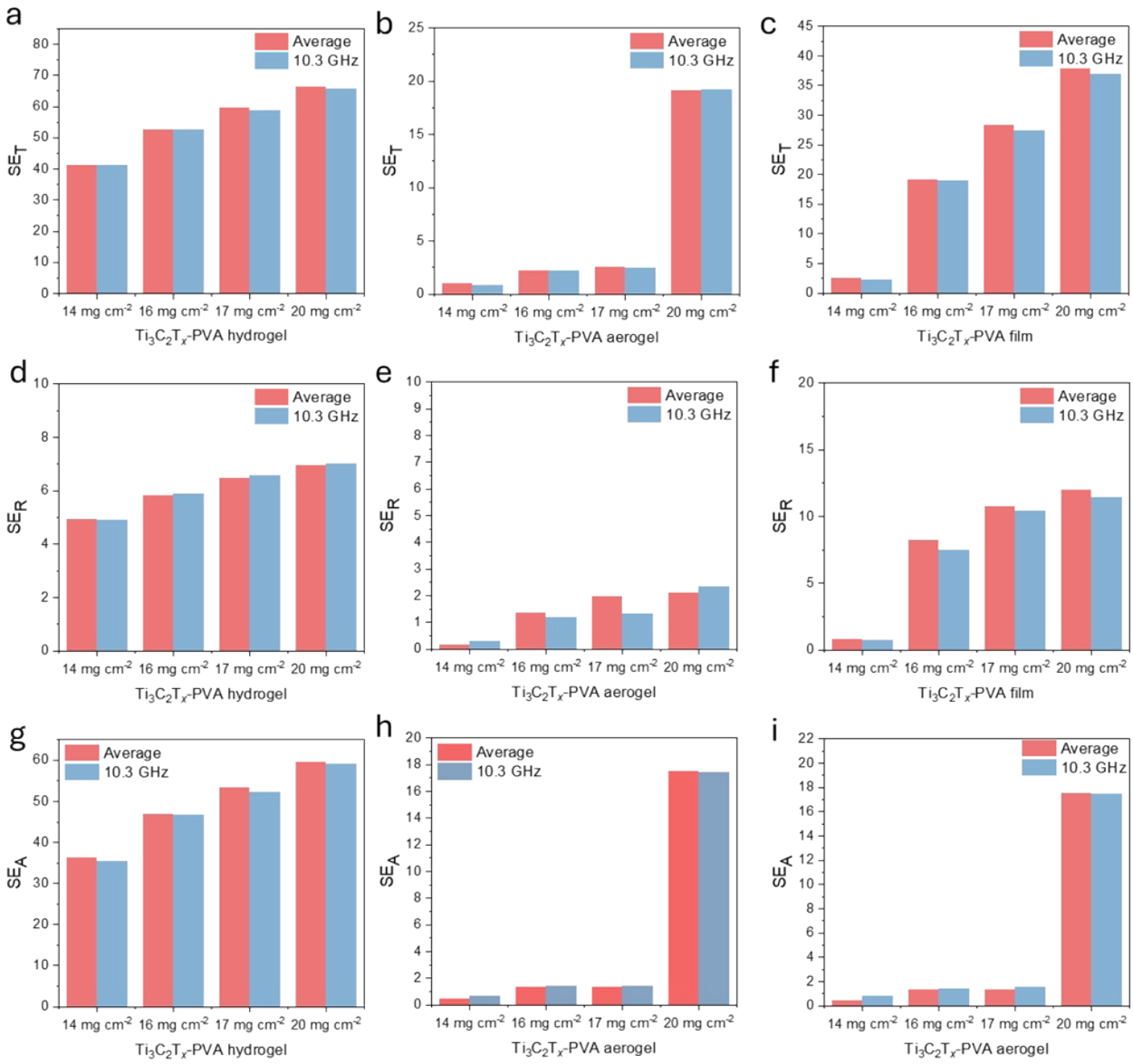

Figure S14. Comparison between average EMI shielding parameters and EMI shielding parameters from 10.3 GHz SE_T (a-c), SE_R (d-f) and SE_A (g-i).

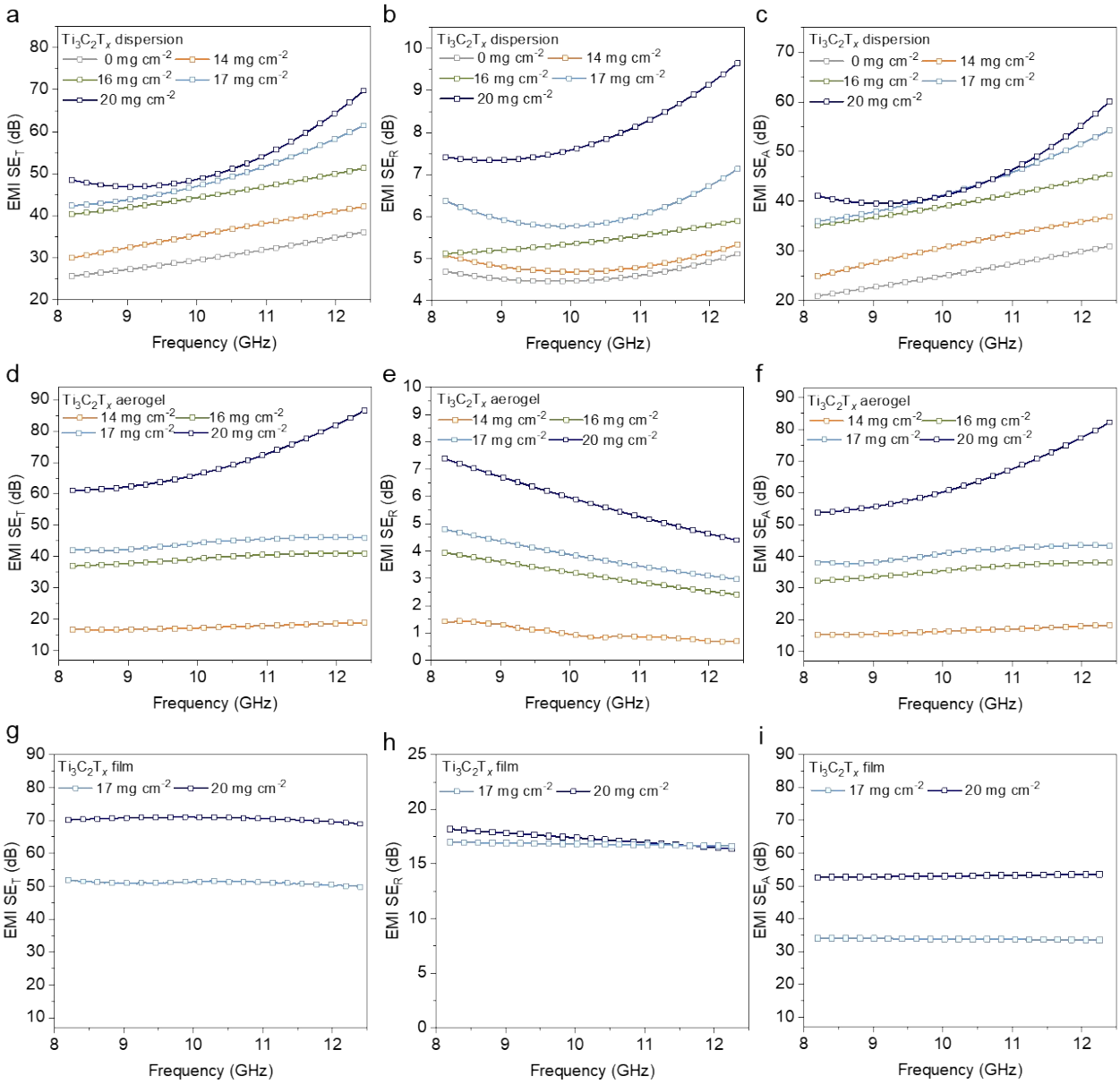

Figure S15. SE_T, SE_R, and SE_A of (a–c) $Ti_3C_2T_x$ dispersions, (d–f) $Ti_3C_2T_x$ aerogels, and (g–i) $Ti_3C_2T_x$ compact films, respectively.

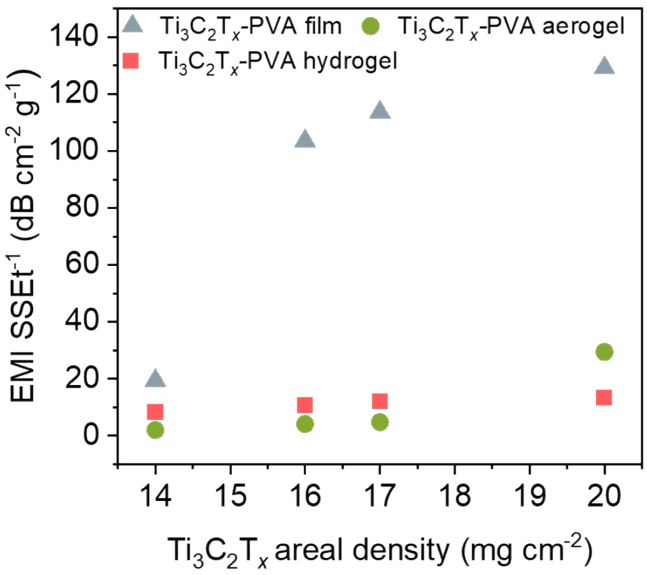

Figure S16. Absolute specific shielding efficiency of $Ti_3C_2T_x$-PVA film, aerogel and hydrogel with respect to $Ti_3C_2T_x$ areal density.

Table S1. Thickness, density, tensile strength, elongation at break, Young's modulus and ionic/ electrical conductivity for $Ti_3C_2T_x$-PVA hydrogels, aerogels, and compact films.

Sample	Thickness (mm)	ρ (g cm^{-3})	Tensile/ compressive strength (MPa)	Elongation at break (%)	Young's modulus (GPa)	Ionic conductivity/ electrical conductivity (S cm^{-1})
Hydrogels						
PVA hydrogel	5±0.02	0.99±0.01	2.48±0.01	417.29±2	3.51 x 10^{-3}	4.98 x 10^{-4}*
$Ti_3C_2T_x$-PVA hydrogel (14 mg cm^{-2})	5±0.02	1.01±0.01	4.83±0.02	636.45±2	6.62 x 10^{-3}	5.08 x 10^{-4}*
$Ti_3C_2T_x$-PVA hydrogel (20 mg cm^{-2})	5±0.02	1.02±0.02	3.44±0.01	507.81±1	5.91 x 10^{-3}	3.89 x 10^{-4}*
$Ti_3C_2T_x$ dispersion (20 mg cm^{-2})	5±0.02	1.03±0.01	-	-	-	2.35 x 10^{-4}*
Aerogels						
PVA-aerogel	5±0.02	0.10±0.01	129.21 x 10^{-3}	50.01±0.01	1.13 x 10^{-7}	~1 x 10^{-13}
$Ti_3C_2T_x$-PVA aerogel (14 mg cm^{-2})	5±0.01	0.11±0.01	215.32 x 10^{-3}	50.01±0.01	6.3 x 10^{-5}	2.62 x 10^{-8}
$Ti_3C_2T_x$-PVA aerogel (20 mg cm^{-2})	5±0.01	0.14±0.01	113.17 x 10^{-3}	50.01±0.01	2.4 x 10^{-5}	1.98 x 10^{-3}
$Ti_3C_2T_x$ aerogel (20 mg cm^{-2})	5±0.01	0.04±0.01	1.06 x 10^{-3}	50.00±0.01	6.0 x 10^{-8}	1.1
Compact films						
PVA-film	9.5 x 10^{-2}	1.16±0.02	32.53±0.2	107.52±0.02	1.6±0.01	~1.1 x 10^{-12}
$Ti_3C_2T_x$-PVA film (14 mg cm^{-2})	11.5 x 10^{-2}	1.17±0.02	55.04±0.3	65.5±0.05	2.1±0.02	9.20 x 10^{-8}
$Ti_3C_2T_x$-PVA film (20 mg cm^{-2})	18.1 x 10^{-2}	1.62±0.02	31.89±0.2	13.96±0.04	6.1±0.03	3.42 x 10^{-2}
$Ti_3C_2T_x$ film (20 mg cm^{-2})	9 x 10^{-3}	3.83±0.01	29.38±0.1	0.37±0.001	9.2±0.01	10,000

*Ionic conductivity (S cm^{-1})